Conditions of predominant occurrence of catalytic reduction of O-2 by ferrous hemin over formation of ferrous hemin-O-2 adduct

Journal of Electroanalytical Chemistry 743 (2015) 134–138

Conditions of predominant occurrence of catalytic reduction of O_2 by ferrous hemin over formation of ferrous hemin-O_2 adduct

Wenwen Li, Koichi Jeremiah Aoki, Jingyuan Chen *, Toyohiko Nishiumi

Department of Applied Physics, University of Fukui, 3-9-1 Bunkyo, Fukui 910-0017, Japan

ARTICLE INFO

Article history:
Received 31 October 2014
Received in revised form 13 February 2015
Accepted 18 February 2015
Available online 24 February 2015

Keywords:
Catalytic current for the reduction of dioxygen by adsorbed hemin
Dioxygen adduct of hemin
Spectro-electrochemistry
Stoichiometry of catalytic reaction

ABSTRACT

Hemin, an iron porphyrin, functions as a carriage of dioxygen in mammalian respiration in the ferrous form. It works also as an electrochemical catalyst of the reduction of dioxygen by reproducing the ferrous form from the ferric one. Since the carriage requires stabilization of the dioxygen adduct, the catalytic reduction of dioxygen with the ferric form might hinder the stabilization. This work aims at finding the discrimination between the functions of the carriage and of the catalysis. A hint of the finding lies in the difference between the remarkable catalytic currents in high concentrations of hemin and negligibly small ones in very low concentrations. The catalytic current at the hemin-coated electrode is confirmed to occur at the stoichiometry of two hemin molecules and one dioxygen molecule. When this stoichiometry is applied to the dioxygen adduct of hemin as an intermediate species of the catalysis, high concentrations of dissolved hemin should provide the catalytic current. Spectro-electrochemistry demonstrates that ferrous hemin is not oxidized simply to the ferric form but is converted to other species, e.g. the dioxygen adduct.

1. Introduction

Hemin, iron(III) protoporphyrin IX, not only takes a central role in the redox activity of several heme-proteins [1–3] but also works as an oxygen-carrier for mammalian respiration [4–10] when hemin is built in proteins such as in myoglobin and hemoglobin. Furthermore, it exhibits electrocatalytic properties of detecting hydrogen peroxide [11–19], dioxygen [11,16,20–29], nitrogen oxides [3,12,18,30], superoxides [31], neurotransmitters [32,33] and tryptophan [34]. The redox activity in heme-proteins may be similar to the electrocatalysis from a viewpoint of the combination of chemical reactions with electron transfer steps. In contrast, the carriage of dioxygen is not associated explicitly with the catalysis.

The electrocatalysis of the reduction of dioxygen occurs in the following steps [15,18,20,26,29]: ferric hemin is reduced electrochemically at the potential at which dioxygen is not reduced; the generated ferrous hemin reduces dioxygen to be retrieved to the ferric form, which induces the reduction current. In contrast, it is ferrous hemin that transports dioxygen in mammalian respiration as an adduct of dioxygen rather than ferric hemin [4–9]. The stability of the adduct has been explained in terms of the steric effects [8,10,35,36]. The formation of the adduct does not lead directly to the catalytic mechanism, in that ferrous hemin encountering dioxygen is converted to the ferric type to lose the ability of the carriage. If ferrous hemin generates adducts of dioxygen, the catalytic reaction should be blocked. If ferric hemin causes the catalytic reaction, on the other hands, the adduct is less formed [37]. There may be specific conditions under which the catalytic reaction competes with the formation of the adduct. Here, we compare the catalytic effects of dioxygen at adsorbed hemin with those in dissolved hemin in order to solve the question.

2. Experimental

Hemin (Wako) with nominal 97% purity was stored in a refrigerator. Dimethyl sulfoxide (DMSO) which was distilled under reduced pressure was dried with molecular sieves. Water was distilled and deionized.

All electrochemical experiments were performed in a three-electrode cell including a Pt wire auxiliary electrode, a reference electrode and the glassy carbon (GC) working electrode of 3 mm in diameter. The reference electrode was a Ag/Ag^+ (0.010 M (=mol dm^{-3}) $AgNO_3$) for DMSO solution or a Ag|AgCl (3.5 M KCl) electrode for phosphate buffer solution 0.20 M, pH 7.4 (25 °C). When hemin-included DMSO solution was dropped on the GC electrode, it dispersed uniformly not only to the GC electrode but also to the insulating wall made of polyetherketone of

* Corresponding author.
E-mail address: jchen@u-fukui.ac.jp (J. Chen).

6 mm in diameter. The ring-shaped boundary of the drop was on the outer edge of the insulating wall. The image of the coated electrode surface was uniform. The actual amount of hemin on the electrode was calculated by multiplying $(3\ \text{mm}/6\ \text{mm})^2$. A potentiostat used was Compactstat (Ivium, Netherlands).

Spectro-electrochemical measurements was made with V-570 UV/VIS/NIR Spectrophotometer (Jasco, Japan) by use of a thin layer cell made of quartz 0.47 mm thick, into which the Pt mesh $0.076 \times 50 \times 10\ \text{mm}^3$ with the density 80 lines per inch was inserted [37].

3. Results and discussion

3.1. Catalytic current for the reduction of dioxygen

Fig. 1(a) shows voltammograms in deaerated phosphate buffer solution 0.20 M, pH 7.4 (25 °C) at the GC electrode coated with the hemin film, where 30 μm^3 DMSO solution including 0.010 mM hemin, i.e. 0.30 nmol hemin was dispersed on the electrode and was dried at 60 °C. The reduction and the oxidation peaks appeared at −0.37 V and −0.22 V vs. Ag|AgCl, respectively. Since the cathodic peak currents were proportional to the scan rate, v, for $0.05 < v < 1.0\ \text{V s}^{-1}$, the current originates in the surface reaction of the adsorbed ferric hemin. When air was bubbled in the solution, the reduction peak current was enhanced, as shown in Fig. 1(b). Then the oxidation peak disappeared, indicating that hem(Fe^{2+}) should be consumed by fast complicated chemical reaction processes. In contrast, dioxygen was reduced at the bare GC electrode at the potential 0.55 V more negative than the reduction of hemin (Fig. 1(c)). Consequently the enhanced current at −0.30 V vs. Ag|AgCl by the air bubbling can be regarded as the catalytic current of dioxygen by hemin. When dioxygen gas under 1 atm was bubbled in the solution, the peak current at the hemin-coated electrode increased 5 times larger than the current by air. This result supports the electrocatalysis of dioxygen.

The electric charge density was evaluated from (i) drawing a background line along the cathodic wave of Fig. 1(a) at −0.7 V and 0.1 V, (ii) integrating the domain encircled with the wave and the background line, (iii) dividing the area by the scan rate, and (iv) dividing the resulting charge by the geometrical area of the electrode. It was $1.5 \times 10^{-10}\ \text{mol cm}^{-2}$. It corresponds to the area $(1.0\ \text{nm})^2$ per adsorbed hemin molecule if hemin is adsorbed uniformly on the electrode. If surface roughness (ranging from 2 to 5 supposedly as used conventionally for electrode surfaces) is taken into account, the area per adsorbed hemin molecule is close to the projected area of the molecule with a flat-lying orientation. According to the model of catalysis caused by adsorbed species [38], the reaction rate is assumed to have a linear relation with the surface concentration, Γ, of the adsorbed species. In order to examine this assumption, we obtained variations of the catalytic peak currents at −0.3 V vs. Ag|AgCl with surface concentrations of hemin, as shown in Fig. 2. The peak current did not vary with Γ for $\Gamma < 10^{-8}\ \text{mol cm}^{-2}$. Therefore the adsorbed concentration of ferric hemin is large enough for the consumption of dioxygen. Even the thinnest film, $\Gamma = 1.1 \times 10^{-12}\ \text{mol cm}^{-2}$ corresponding to the area $(12\ \text{nm})^2$ per adsorbed hemin molecule, did not suppress the catalytic current. If this surface concentration were to be layered with each 12 nm separation, the volume concentration of hemin would become 0.9 mM. This concentration is still larger than the concentration of dioxygen saturated by air, 0.5 mM. As a result, the catalytic current is not controlled by surface concentrations of hemin for $10^{-12} < \Gamma < 10^{-8}\ \text{mol cm}^{-2}$. The peak current should vanish as Γ tends to zero. It was difficult to decrease Γ less than $10^{-12}\ \text{mol cm}^{-2}$ reproducibly, because of dependence on the preparation processes of the solution. The ill reproducibility for the lower concentrations may be caused by adsorption of hemin on vessels. On the other hands, the catalytic current decreased with an increase in the surface concentration for $\Gamma > 7.4 \times 10^{-9}\ \text{mol cm}^{-2}$. The thick films obviously block the transport of the charge in the film, and hence suppress the current.

Fig. 3 shows dependence of (a) the catalytic peak potentials, E_p, and (b) the reduction peak potentials at the bare GC electrode on the logarithmic scan rates. The comparison between the two indicates that the catalytic reaction decreases the overpotential by 0.5–0.6 V. Both plots fall each line, the slope of which are −0.035 V and −0.10 V for the catalysis and the direct reduction, respectively. The peak potentials of the catalytic currents are close to those of the reduction peak of adsorbed hemin without dioxygen (c), where the determination of the latter contained errors ca. 0.03 V. The similarity indicates that the catalytic potential shift (a) by the scan rate should be caused by the potential shift of adsorbed hemin (c). In other words, the catalytic current itself does not provide any potential shift by the scan rates.

Fig. 4(a) shows variations of the catalytic peak current with the square-roots of the scan rate. Since the currents were proportional to $v^{1/2}$, they ought to be controlled by diffusion of dioxygen. In contrast, the reduction peak currents at the GC bare electrode (b) were not only unproportional to $v^{1/2}$, but also were smaller than half the catalytic currents (a). They may be associated with chemical complications rather than diffusion [39]. Some complications are

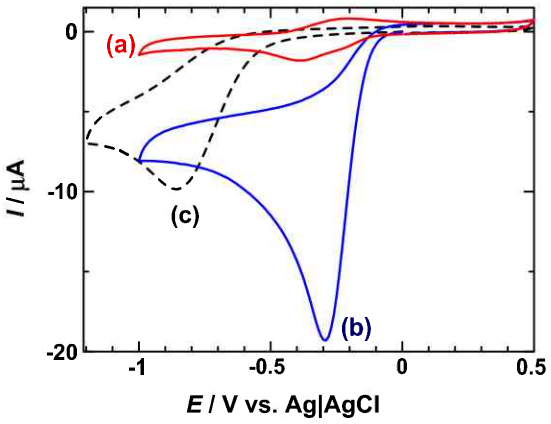

Fig. 1. Voltammograms at the hemin-coated GC electrode in (a) deaerated and (b) aerated phosphate buffer solution 0.20 M, pH 7.4 (25 °C) for $v = 0.1\ \text{V s}^{-1}$, where a drop of 30 μm^3 with 0.010 mM (M = mol dm^{-3}) hemin, corresponding to 0.30 nmol hemin, was cast on the electrode. Voltammogram (c) is at the bare GC electrode in the aerated solution.

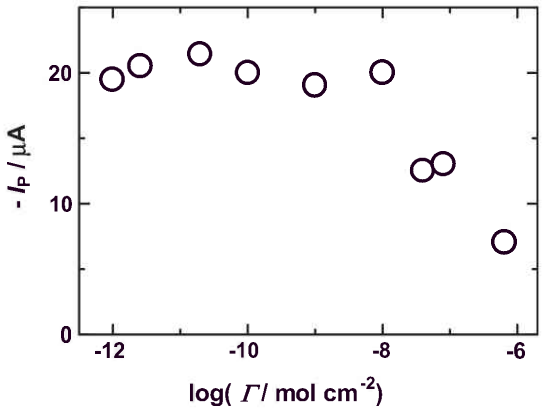

Fig. 2. Dependence of the catalytic peak currents on the molar density of adsorbed hemin, observed in aerated phosphate buffer solution, 0.20 M pH 7.4 (25 °C) at the GC electrode.

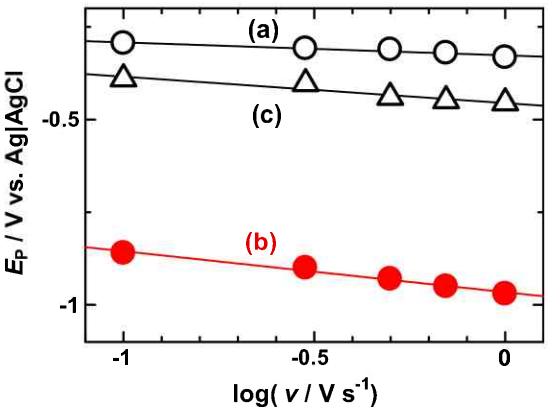

Fig. 3. Variations of the cathodic peak potentials with the logarithmic scan rates at the hemin-coated electrode ($\Gamma = 1.1 \times 10^{-9}$ mol cm^{-2}) in the (a) aerated and (c) deaerated phosphate buffer solution 0.2 M, pH 7.4 (25 °C). The peak potentials (b) were obtained at the bare GC electrode in the aerated solution.

supported by the large variation of E_p vs. log v in Fig. 3(b). The slope of the proportional line in Fig. 4(a), 49 μA V$^{-1/2}$ s$^{1/2}$, is close to the slope value, 42 μA V$^{-1/2}$ s$^{1/2}$, calculated from the equation for the diffusion controlled current at the successive two-electron transfer reaction ($n = 2$) [40],

$$I_p = -0.446nFAc^*(DvF/RT)^{1/2} \quad (1)$$

where the concentration of dioxygen by air saturation c^* was 0.5 mM at 25 °C, the diffusion coefficient of dioxygen D was 1.96×10^{-5} cm^2 s^{-1} [41], and A is the electrode area. Eq. (1) is different from the well-documented expression by $n^{3/2}$. The approximate agreement between the experimental value of I_p and Eq. (1) indicates that dioxygen can be quantitatively determined by hemin-coated electrodes only when $\Gamma < 10^{-9}$ mol cm^{-2}.

The electron transfer number, two, suggests the following reaction mechanisms:

$$O_2 + 2\text{hem}(Fe^{2+}) \rightarrow O_2^{2-} + 2\text{hem}(Fe^{3+}) \quad (2)$$

$$2\text{hem}(Fe^{3+}) + 2e^- \rightarrow 2\text{hem}(Fe^{2+}) \quad (3)$$

The reported values of n for the catalytic reduction of dioxygen by hemin are one [18], two [15] and four [20,26]. The stoichiometry $n = 2$ cannot be realized in the adsorbed hemin layer, in which the number of hemin molecules are much larger than of dioxygen molecules.

3.2. Reaction of dissolved hemin with dioxygen

The hemin-dissolved DMSO solution showed only the diffusion-controlled current of hemin at the platinum or the gold electrode without any catalytic reaction [37]. In contrast, the GC electrode at which hemin was naturally adsorbed exhibited a small contribution of the catalytic currents for the reduction of dioxygen [37]. The catalytic peak currents for $v < 0.07$ V s^{-1} were proportional to $v^{1/2}$, whereas those for $v > 0.10$ V s^{-1} were larger than the proportional line. The latter can be approximately expressed by $-I_p = k_1 v^{1/2} + k_2 v$ for positive constants, k_1 and k_2. The approximation was valid independently of the time during which the GC electrode was immersed into the hemin + DMSO solution. The amount of the adsorption estimated from the value of k_2 was 5×10^{-9} mol cm^{-2} if the ideal waveform for the adsorption is valid [37]. Since this amount is much larger than 10^{-12} mol cm^{-2}, the condition of causing the catalysis is satisfied. The catalysis seems to require (A) water in solution and (B) adsorbed hemin rather than dissolve hemin. In order to examine (A), we made voltammetry in the aerated DMSO solution to which water was added gradually at the vol/vol ratios from 0.01 to 0.5. When water was added to the DMSO + hemin solution, the mixture turned transparent, exhibiting turbid red-brown sediment. With an increase in the water ratio, the reduction peak currents decreased owing to a loss of solubility of hemin. They were proportional to $v^{1/2}$, independent of addition of water, with and without dioxygen. These observations agreed with the same catalytic behavior that was observed at low hemin concentrations in DMSO. This fact proves that water does not cause the catalysis. Condition (B) implies a property of an adsorbed state different from a dissolved state. A possible property as to the difference is concentration. We increased concentrations of dissolved hemin in DMSO to see whether the reduction current included a catalytic component or not. Fig. 5 shows the voltammograms of concentrated hemin in aerated DMSO at the Pt electrode. The voltammetric shape was close to that in the aqueous solution at hemin-adsorbed GC electrode in Fig. 1. The reduction peak currents were proportional to $v^{1/2}$. They are plotted against hemin concentrations in Fig. 6. The currents for concentrations less than 0.5 mM were proportional to the concentrations on hemin and $v^{1/2}$, indicating the diffusion control [37]. Those for concentrations over 0.7 mM had a quadratic relation with the concentration, as shown in the dashed curve in Fig. 6. The component over the proportional line should be due to the catalysis. The peak currents without dioxygen were proportional to the concentration of hemin lower than 2 mM, and were controlled by diffusion of hemin.

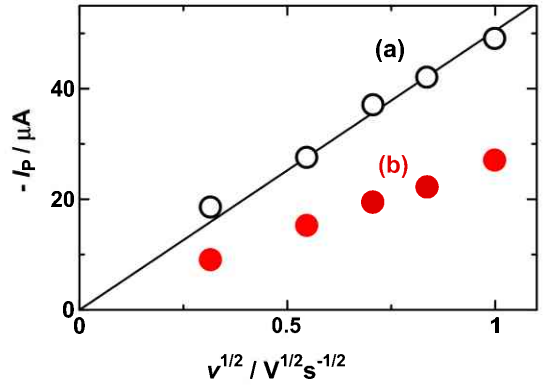

Fig. 4. Dependence of the cathodic peak currents of dioxygen at (a) the hemin-coated GC electrode and (b) the bare GC electrode on the square-roots of the scan rates, where dioxygen was supplied from air.

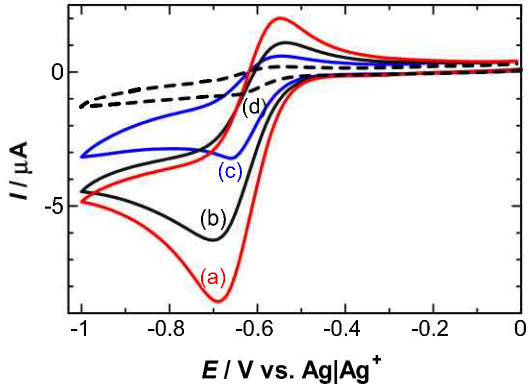

Fig. 5. Voltammograms in several concentrations of hemin with (a) 2.0, (b) 1.5, (c) 1.0, and (d) 0.3 mM at the Pt electrode for $v = 0.1$ V s^{-1} in the aerated DMSO including 0.15 $TBAClO_4$.

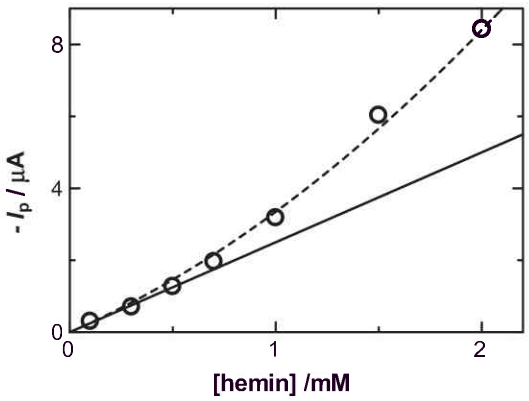

Fig. 6. Variation of the cathodic peak current with the concentration in Fig. 5. The dotted curve is fitted to $-I_p = 2.5\ [\text{hemin}] + 0.85\ [\text{hemin}]^2$.

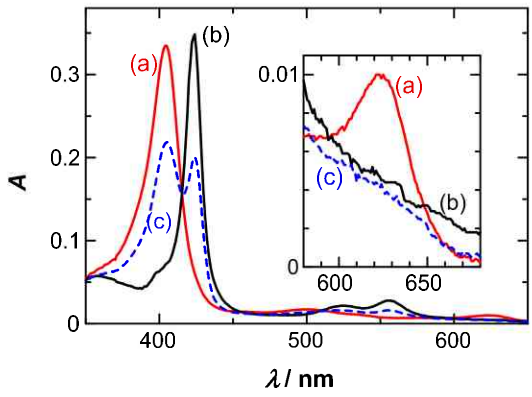

Fig. 7. UV–vis spectra of (a) hem(Fe^{3+}), (b) hem(Fe^{2+}) and (c) dioxygen-added hem(Fe^{2+}) for 30 s in the UV-electrochemical, thin layer cell including 0.032 mM hemin + DMSO. The thickness of the cell was 0.4 mm into which the platinum mesh-electrode (150 mesh) was inserted. The reduction was made at −0.6 V vs. Ag|AgCl for 10 min.

We consider tentatively the dioxygen adduct of hemin as

$$O_2 + 2\text{hem}(Fe^{2+}) \leftrightarrow (\text{hem}(Fe^{2+}))_2O_2 \quad (4)$$

The stability constant for $(\text{hem}(Fe^{2+}))_2O_2$ is expressed by

$$K = [(\text{hem}(Fe^{2+}))_2O_2]/[O_2][\text{hem}(Fe^{2+})]^2 \quad (5)$$

If the adduct is decomposed through

$$(\text{hem}(Fe^{2+}))_2O_2 \rightarrow O_2^{2-} + 2\text{hem}(Fe^{3+}) \quad (6)$$

the catalytic current is observed, which is controlled by the decomposition rate of the adduct, i.e. $k_d[(\text{hem}(Fe^{2+}))_2O_2]$, where k_d is the decomposition rate constant. Since the observed current in the aerated solution of dissolved hemin is the sum of the catalytic current and the diffusion controlled current, the substitution of [hem(Fe^{2+})] for $[(\text{hem}(Fe^{2+}))_2O_2]$ by use of Eq. (5) yields

$$-I_p = 0.446FAc^*(D\upsilon F/RT)^{1/2} + k_dK[O_2][\text{hem}(Fe^{2+})]^2 \quad (7)$$

where c^* is the bulk concentration of hem(Fe^{3+}). Since the redox reaction of hemin is reversible, the term [hem(Fe^{2+})] in the second term can be approximated as c^*. As a result, Eq. (7) is reduced approximately as

$$-I_p = 0.446FAc^*(D\upsilon F/RT)^{1/2} + k_dK[O_2]c^{*2} \quad (8)$$

Then the current is expressed by a quadratic equation of hemin concentration, as can be demonstrated by Fig. 6. Concentrations of dissolved species for voltammetry are usually less than 1 mM, whereas those for adsorbed species are more than a few molarities. Therefore the second term in Eq. (7) for the adsorbed hemin is larger by 10^6–10^8 larger than that for the dissolved hemin. This estimation explains the appearance of the catalysis at the hemin-coated electrode.

We try to find formation of the dioxygen adduct in reaction (4) spectroscopically under our experimental conditions without any enzymatic support. Ferrous hemin was generated electrochemically at the platinum mesh electrode in a thin layer cell through which a monochromatic beam was passed. Fig. 7 shows UV–vis spectra for (a) ferric hemin and (b) electrochemically reduced hemin. Ferric and ferrous hemins show the Soret band at 404 nm and 424 nm, respectively, being close to bibliographic values [10,35,42–45]. As hemin(Fe^{3+}) was reduced electrochemically, the absorbance at 424 nm increased at the expense of the absorbance at 404 nm. When dioxygen was added to the hemin(Fe^{2+}) solution after the sufficiently cathodic electrolysis, the absorbance at 404 nm was partially restored, implying the oxidation of the ferrous ion by dioxygen into ferric ion. However, the band at 404 nm is overlapped with the species generated when dioxygen is added to hem(Fe^{2+}) [42,44]. Since the band at 424 nm is specific to hem(Fe^{2+}), it is obvious that purging dioxygen to the hem(Fe^{2+}) solution decreased the concentration of hem(Fe^{2+}) by a half (c). The enhancement of the absorbance at 404 nm can be attributed either to the hem(Fe^{3+}) or the dioxygen adduct. The Q bands are the other measure of redox states of hemin in the wavelengths ranging from 500 to 650 nm although the absorbance coefficients are small. The inset of Fig. 7 shows the bands at 621 nm for hem(Fe^{3+}), which is specific to hem(Fe^{3+}) discriminating against hem(Fe^{2+}) [44,46]. The addition of dioxygen to hem(Fe^{2+}) did not exhibit the band at 621 nm. This result indicates that hem(Fe^{2+}) should not be oxidized simply to hem(Fe^{3+}) but be converted to other species, e.g. the dioxygen adduct, which is detected at 404 nm. This is a confirmation of reaction (4).

When the reduction potential of hemin is applied to the electrode, hem(Fe^{3+}) near the electrode is consumed by the electrode reaction. Then the forward rate in Eq. (7) increases to depress $[(\text{hem}(Fe^{2+}))_2O_2]$. As a result, the adduct has not been recognized in electrochemically catalytic experiments.

4. Conclusions

The catalytic current for the reduction of dioxygen at the hemin-coated electrode is controlled by diffusion of dioxygen at the reduced potential of hem(Fe^{3+}) with successive two-electron reduction, independent of surface concentrations of hemin for $10^{-12} < \Gamma < 10^{-9}$ mol cm^{-2}. The diffusion-controlled step without essential potential shift indicates that any reaction rate constant in Eq. (2) cannot be evaluated from the present voltammetric data. The catalytic current is not observed at the bare Pt electrode in hemin-dissolved solution for [hem(Fe^{3+})] < 0.5 mM, but it can be for [hem(Fe^{3+})] > 1 mM. The catalytic current is proportional to the quadratic relation of hemin concentrations. The quadratic relation can be ascribed to the stoichiometry of the reaction of two ferrous hemin molecules with one dioxygen molecule to generate the dioxygen adduct.

The dioxygen adduct can be regarded as an intermediate of the catalytic reaction, given by reaction (4). It is decomposed to generate hem(Fe^{3+}) by Eq. (6), which is reduced electrochemically to yield the catalytic current. As the electrochemical reduction proceeds, [hem(Fe^{3+})] decreases electrochemically at the expense of the adduct. Therefore the adduct is not directly detected by voltammetric measurements.

Conflict of interest

There is no conflict of interest among authors.

Acknowledgment

This work was financially supported by Grants-in-Aid for Scientific Research (Grant 25420920) from the Ministry of Education in Japan.

References

[1] J. Xie, X. Feng, J. Hu, X. Chen, A. Li, Biosens. Bioelectr. 25 (2010) 1186–1192.
[2] N. Jia, Y. Wen, G. Yang, Q. Lian, C. Xu, H. Shen, Electrochem. Commun. 10 (2008) 774–777.
[3] K. Liu, J. Zhang, G. Yang, C. Wang, J.-J. Zhu, Electrochem. Commun. 12 (2010) 402–405.
[4] K. Imai, J. Mol. Biol. 133 (1979) 233–247.
[5] M. Brunori, R.W. Noble, E. Antonini, J. Wyman, J. Biol. Chem. 241 (1966) 5238–5243.
[6] M.H. Keyes, M. Falley, R. Lumry, J. Am. Chem. Soc. 93 (1971) 2035–2040.
[7] J.P. Collman, J.I. Brauman, K.S. Suslick, J. Am. Chem. Soc. 97 (1975) 7185–7186.
[8] J.P. Collman, J.I. Brauman, K.M. Doxsee, T.R. Halbert, K.S. Suslick, Proc. Natl. Acad. Sci. 75 (1978) 564–568.
[9] C.-Z. Li, G. Liu, S. Prabhulkar, Am. J. Biol. Sci. 1 (2009) 303–311.
[10] T.G. Traylor, Acc. Chem. Res. 14 (1981) 102–109.
[11] L. Shen, N. Hu, Biochim. Biophys. Acta 1608 (2004) 23–33.
[12] F. Valentini, L. Cristofanelli, M. Carbone, G. Palleschi, Electrochim. Acta 63 (2012) 37–46.
[13] G.L. Turdean, I.C. Popescu, A. Curulli, G. Palleschi, Electrochim. Acta 51 (2006) 6435–6441.
[14] Q. Yang, Y. Nie, X. Zhu, X. Liu, G. Li, Electrochim. Acta 55 (2009) 276–280.
[15] Y. Gao, J. Chen, J. Electroanal. Chem. 578 (2005) 129–136.
[16] J. Chen, L. Zhao, H. Bai, G. Shi, J. Electroanal. Chem. 657 (2011) 34–38.
[17] Y. Guo, J. Li, S. Dong, Sens. Actuat. B 160 (2011) 295–300.
[18] Q.-L. Sheng, J.-B. Zheng, X.D. Shang-Guan, W.-H. Lin, Y.-Y. Li, R.-X. Liu, Electrochim. Acta 55 (2010) 3185–3191.
[19] H. Hong, J. Porous Mater. 13 (2006) 393–397.
[20] F. Arifuku, K. Mori, T. Muratani, H. Kurihara, Bull. Chem. Soc. Jpn. 65 (1992) 1491–1495.
[21] H. Iken, L. Etcheverry, A. Bergel, R. Basseguy, Electrochim. Acta 54 (2008) 60–65.
[22] R. Jiang, D.T. Tran, J.P. McClure, D. Chu, Electrochim. Acta 75 (2012) 185–190.
[23] J.B. Xu, T.S. Zhao, L. Zeng, Int. J. Hydrogen Energy 37 (2012) 15976–15982.
[24] Z.X. Liang, H.Y. Song, S.J. Liao, J. Phys. Chem. C 115 (2011) 2604–2610.
[25] P.-B. Xi, Z.-X. Liang, S.-J. Liao, Int. J. Hydrogen Energy 37 (2012) 4606–4611.
[26] N. Zheng, Y. Zen, P.G. Osbore, Y. Li, W. Chang, Z. Wang, J. Appl. Electrochem. 32 (2002) 129–133.
[27] P.-J. Wei, G.-Q. Yu, Y. Naruta, J.-G. Liu, Angew. Chem., Int. Ed. 53 (2014) 6659–6663.
[28] L. Liu, F. Zhao, F. Ma, L. Zhang, S. Yang, N. Xia, Biosens. Bioelectr. 49 (2013) 231–235.
[29] J. Collman, R. Boulatov, Angew. Chem. Int. Ed. 41 (2002) 3487–3489.
[30] M.T. de Groot, M. Merkx, A.H. Wonders, M.T.M. Koper, J. Am. Chem. Soc. 127 (2005) 7579–7586.
[31] J. Chen, U. Wollenberger, F. Lisdat, B. Ge, F.W. Scheller, Sens. Actuators B 70 (2000) 115–120.
[32] B. Duong, R. Arechabaleta, N.J. Tao, J. Electroanal. Chem. 447 (1998) 63–69.
[33] R.-I.S.-van Stadena, I. Moldoveanu, J.F. van Stadena, J. Neuro. Meth. 229 (2014) 1–7.
[34] C.G. Nan, Z.Z. Fena, W.X. Li, D.J. Ping, C.H. Qin, Anal. Chim. Acta 452 (2002) 245.
[35] T.G. Traylor, S. Tsuchiya, D. Campbell, M. Mitchell, D. Stynes, N. Koga, J. Am. Chem. Soc. 107 (1985) 604–614.
[36] J.S. Olson, R.F. Eich, L.P. Smith, J.J. Warren, B.C. Knowles, Biotechnology 25 (1997) 227–241.
[37] K.J. Aoki, W. Li, J. Chen, T. Nishiumi, J. Electroanal. Chem. 713 (2014) 131–135.
[38] K. Aoki, K. Tokuda, H. Matsuda, J. Electroanal. Chem. 199 (1986) 69–79.
[39] H. Zhang, K. Aoki, J. Chen, T. Nishiumi, H. Toda, E. Torita, Electroanalysis 23 (2011) 947–952.
[40] K. Aoki, Electroanalysis 17 (2005) 1379–1383.
[41] P. Han, D.M. Bartels, J. Phys. Chem. 100 (1996) 5597–5602.
[42] G.C. Chu, K. Katakura, X. Zhang, T. Yoshida, J. Biol. Chem. 274 (1999) 21319–21325.
[43] T. Komatsu, Y. Matsukawa, E. Tsuchida, Bioconjugate Chem. 13 (2002) 397–402.
[44] M. Couture, T.K. Das, P.-Y. Savard, Y. Ouellet, J.B. Wittenberg, B.A. Wittenberg, D.L. Rousseau, M. Guertin, Eur. J. Biochem. 267 (2000) 4770–4780.
[45] T. Komatsu, N. Ohmichi, P.A. Zunszain, S. Curry, E. Tsuchida, J. Am. Chem. Soc. 126 (2004) 14304–14305.
[46] H. Durliat, M. Comtat, J. Biol. Chem. 262 (1987) 11497–11500.